

Synthesis of Fluorinated and Hydrocarbon Ester Functionalized Poly(*p*-phenylenes) and Their Solubility in Supercritical Fluids

Michael E. Wright,^{*,†} Kimberly M. Lott,[‡] Mark A. McHugh,^{*,‡} and Zhihao Shen[‡]

Chemistry & Materials Division, NAWCWD, China Lake, California 93555-6100, and Departments of Chemistry and Chemical Engineering, Virginia Commonwealth University, Richmond, Virginia 23284

Received October 23, 2002; Revised Manuscript Received January 28, 2003

ABSTRACT: Monomers of the structure 2,5-dichloro-1,4-(RO₂C)₂benzene, where R = CH₂CF₂CF₃ (**1a**), -(CH₂)₂CH₃ (**1b**), -CH₂CH₂(CF₂)₅CF₃ (**1c**), and -(CH₂)₇CH₃ (**1d**), were prepared and characterized in the study. Polymerization by the Ni-catalyzed/Zn-mediated homocoupling methodology afforded poly(*p*-phenylenes) **2a–2d**. The polymers obtained after precipitation into methanol showed molecular weights (*M_n*, relative to polystyrene standards) in the range 7000–13 000. The regiochemistry in the polymer was deduced to be approximately 70% head-to-tail with the remainder head-to-head. The polymers displayed excellent solubility in common polar organic solvents such as THF and chloroform. The poly(*p*-phenylenes) **2a** and **2b** showed no solubility in supercritical ethane, propane, butane, and carbon dioxide even at 190 °C and 35 000 psia. Polymer **2d** was remarkably soluble in the supercritical hydrocarbon solvents at low pressures (1000 psia). However, **2d** does not dissolve in supercritical carbon dioxide. The fluorinated poly(*p*-phenylene) **2c** dissolved in the supercritical hydrocarbons at pressures below 6000 psia, and it dissolved in carbon dioxide at pressures as low as 1000 psia at 25 °C.

Introduction

For the past several decades polymer chemists have been interested in the unique properties of poly(*p*-phenylene) (PPP)-based materials that are a consequence of the “linear and rigid backbone” chain architecture of PPP.¹ The outstanding thermal stability of PPP motivated much of the early research efforts to focus on the synthesis of processable derivatives of PPP.² Within the past decade, there has been increased attention directed at designing highly functionalized and processable poly(phenylenes) due to the many high-performance applications proposed for these type of polymers.³ Functionalized poly(phenylenes) are now readily synthesized in high yields and often as high molecular weight materials by homo- or cross-coupling reactions that are typically nickel- or palladium-catalyzed.⁴ Functionalization of the PPP backbone is necessary to ensure polymer solubility for synthesis as well as for the later processing of these materials. However, the backbone functional groups can be chemically modified or even completely removed at a later stage. For example, Kaeriyama and co-workers generated an ester functionalized PPP from the nickel-catalyzed/zinc-mediated homo-coupling of methyl 2,5-dichlorobenzoate,⁵ isolated the PPP, hydrolyzed the ester groups, and then decarboxylated the polymer to produce unsubstituted PPP. Other ester-containing PPPs have been reported in the patent literature⁶ which suggests that PPP-ester-based materials will find greater use in high-performance applications as creative synthesis/solution processing schemes are developed.

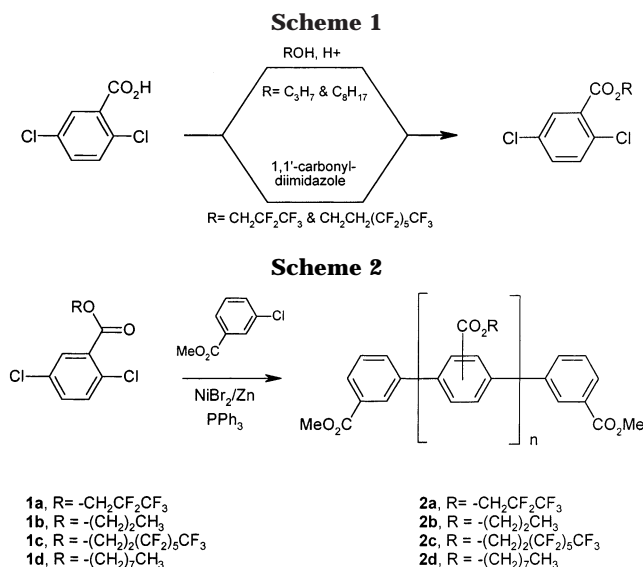
From a fundamental viewpoint, substituted PPPs represent the quintessential architecture to delineate the influence of a substituent group on solubility since unsubstituted PPPs are stiff chain, refractory polymers that do not dissolve in organic liquid solvents. Functionalized PPPs can be very soluble in conventional

liquid organic solvents, which suggests that it may be possible to dissolve and process these polymers in supercritical fluid (SCF) solvents. Several studies have been reported in the past decade or so on the thermodynamics and solution behavior of functionalized, rod-like polymers^{7,8} which provide a template to interpret the polymer–SCF studies reported in the present work. For example, Ballauff reported that polymer crystallization and the possible formation of mesophases of rodlike polymers can be inhibited by a substituent group which acts as a tethered solvent that screens interchain interactions and main chain–solvent interactions and that increases the entropy of dissolution.⁷ Molecular dynamics studies may provide further insight into the role of side chain architecture on the characteristic ratio and persistence length of PPP-type polymers.⁹ It is also important to note that the regioregularity of the main chain has been postulated to affect polymer backbone flexibility that in turn could influence solubility.⁹ Hence, the chemical architecture of the side chains and the regioregularity of the main chain are both expected to have a strong influence on the pressures and temperatures needed to dissolve substituted PPPs in SCF solvents.

The present study reports the synthesis of new, fluorinated and nonfluorinated, propyl and octyl ester functionalized PPPs. The role of the ester side chain on the solubility of derivatized PPPs is investigated as a function of the alkoxy tail length and its fluorine content. The polarity of the ester group will remain relatively constant in the examples studied. The supercritical fluids of interest are CO₂, ethane, propane, and butane. In general, the level of polymer solubility in supercritical CO₂ is sensitive to polarity and backbone flexibility.^{10,11} It is established that CO₂ does not dissolve nonpolar polyolefins. Hence, fluorinating the alkoxy tail is anticipated to impact solubility for the poly(*p*-phenylenes) on the basis of the observations made with other more flexible polymers.^{12,13} Supercritical alkanes are chosen in this study since these SCF

[†] NAWCWD.

[‡] Virginia Commonwealth University.



solvents readily dissolve nonpolar and slightly polar polyolefins.¹⁴ In this case, the length of the alkoxy tail should again prove to be a controlling variable for solubility since the polarity per molar volume of a molecule decreases as this molar volume increases.¹⁵

Results and Discussion

The alkyl and fluoroalkyl benzoate monomers were synthesized through two different routes (Scheme 1). The alkyl benzoate monomers **1b** and **1d** were synthesized using 2,5-dichlorobenzoic acid and the corresponding alcohol in a Fischer esterification reaction. The fluoroalkyl benzoate monomers were not as easy to synthesize. Low yields were obtained from the Fischer esterification procedures. In addition, treatment of 2,5-dichlorobenzoyl chloride with the fluoro alcohols resulted in complicated product mixtures. Use of dicyclohexylcarbodiimide (DCC) also resulted in a mixture where purification from the resulting urea byproduct proved cumbersome. By far, we achieved our best results using carbonyldiimidazole (CDI) as the coupling agent.¹⁶ The gaseous and water-soluble products (i.e., imidazole) are easily separated from the desired monomer. Isolated yields of the fluoroalkyl monomers were generally above 70% using this procedure.

The polymers used in this study were synthesized as shown in Scheme 2 using the Ni-catalyzed homocoupling chemistry developed by Colon and Kesley.¹⁷ We add a step where the reaction mixture was washed with an aqueous sodium cyanide solution.¹⁸ This was implemented to remove any possible remaining homogeneous nickel complexes that might later become entrapped in a precipitation process. The final polymeric materials after precipitation and drying were fully characterized by analytical and spectroscopic methods. The amount of end cap added to the polymerization reaction was used to help tune the polymer's molecular weight, leading to the four homologous polymers **2a–2d**. Polymer molecular weights were determined by SEC analysis and are reported relative to polystyrene standards.¹⁹ In addition to SEC analysis, the polymer structure was verified and analyzed on the basis of end-group analysis by proton NMR spectroscopy.

The ¹H NMR spectrum of polymer **2d** indicates that the head-to-tail (H–T) and head-to-head (H–H) repeating units are in an approximate ratio of 2. Furthermore,

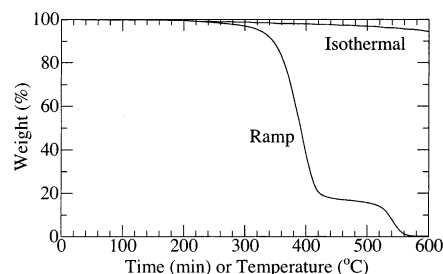


Figure 1. Thermal gravimetric analyses of polymer **2c** were carried out under a nitrogen atmosphere. The isothermal aging study was performed at 250 °C with the *x*-axis in minutes, and for the ramp TGA run (10 °C/min) the axis represents temperature (°C).

two signals are observed in the ¹H NMR spectrum that can be assigned to end cap. One peak at δ 3.95 ppm is assigned to the anticipated end cap, namely methyl benzoate. The second verifiable end cap is assigned to the octyl–ester resonance at δ 4.30 ppm. This latter end cap must arise from a coupling reaction at the 5-chloro position and then either leaving the 2-position unreacted or possibly terminated by reduction (i.e., catalytic replacement chloride by hydrogen). From the integration values we estimate that ~50% of the end groups result from addition of the 3-chlorobenzoate and the remainder belong to reactions involving the monomer and possibly phenyl transfer from the triphenylphosphine ligand during the catalytic process.¹⁷

Polymers **2a–2d** were subjected to thermal analysis using both DSC and TGA instruments. Even though reasonably sized samples (~5 mg) of the polymers can be loaded into DSC sample pans, consistent *T_g* events were not observed. Although small thermal events were observed, especially on the original scan, reproducible (third and fourth scans) events of sufficient magnitude were absent in the scans from –50 to 250 °C. The thermal stability of the polymers was tested using TGA operating in both the isothermal and ramp modes (Figure 1). We find that at 250 °C under a nitrogen atmosphere the polymers show less than ~5% weight loss over a period of 10 h. A decomposition breakpoint of ~350 °C was observed when a sample of **2c** was heated at 10 °C/min under a nitrogen atmosphere. It is interesting to note that no “char residue” remains after the temperature hits ~570 °C.

We have carried out a series of experiments where the octyl 2,5-dichlorobenzoate was polymerized in the presence of varying amounts of end cap. The experiments follow the expected trend by affording a decrease in the *M_n* (number-average molecular weight) as the mol % of end cap added to the reaction mixture is increased (Figure 2).

We have also carried out experiments to determine the relationship of *M_n* as a function of reaction temperature, and the results are depicted in Figure 3. The end cap was maintained at 10 mol % for each temperature studied. As the temperature increased from 70 to 80 °C, there is a notable increase in the *M_n* even though each reaction went to completion. At 90 °C a slight decrease in *M_n* occurs. This is possibly due to catalyst decomposition or to an increase in the rate of competing side reactions such as reduction of the aryl–chloride bond or phenyl transfer from the phosphine ligand. Thus, 80 °C represents an optimized reaction temperature for this monomer and catalyst combination.

The poly(*p*-phenylenes) with fluorinated and non-fluorinated propyl chains (**2a** and **2b**) do not dissolve

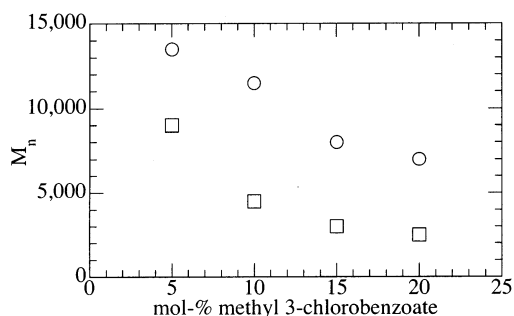


Figure 2. Polymerization of octyl 2,5-dichlorobenzoate as in Scheme 1 but with varying amounts of end cap added to adjust polymer **2d** molecular weight.

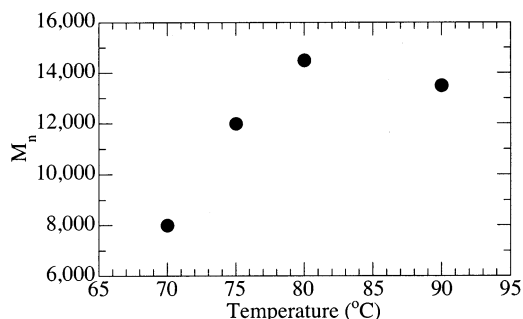


Figure 3. Polymerization of octyl 2,5-dichlorobenzoate carried out at various temperatures. Product **2d** was analyzed by GPC and NMR spectroscopy.

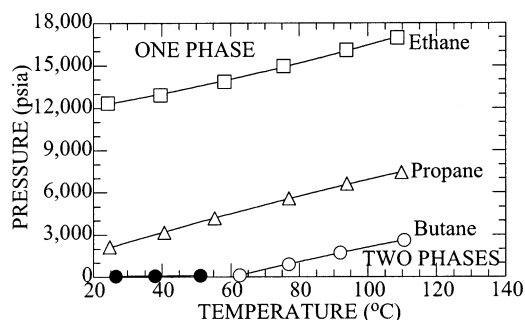


Figure 4. Comparison of the phase boundary curves for 1.3 wt % poly(*p*-phenylene) **2d** in supercritical ethane, propane, and butane. A single phase exists at conditions above each of the curves and two phases exist below the curves. The ethane and propane curves represent cloud points. However, the butane curve represents cloud points (open circles) at temperatures greater than 60 °C and bubble points (filled circles) at lower temperatures. The butane bubble-point pressures are very close to the vapor pressure of pure butane.

in supercritical CO₂, ethane, propane, or butane even at 190 °C and 35 000 psia. Evidently, the alkoxy chains are too short to screen interchain- and main chain-solvent interactions and are not bulky enough to induce chain flexibility as a consequence of steric considerations.⁸ Even when the propyl chains are fluorinated, the side chain-solvent interactions are not large enough to induce dissolution of these rigid-rod polymers in SCF solvents.

Figure 4 shows that poly(*p*-phenylene) **2d** readily dissolves in ethane, propane, and butane, but it does not dissolve in CO₂ even at 135 °C and 35 000 psia. Since ethane, propane, and butane are nonpolar solvents, dispersion interactions are likely to be the dominant type of interaction¹⁵ that fixes the location of the cloud-point curves shown in Figure 4. For example, at 100 °C, the cloud-point pressures decrease from

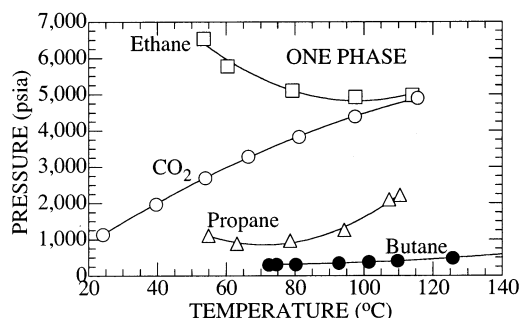


Figure 5. Comparison of the phase boundary curves for 1.3 wt % poly(*p*-phenylene) **2c** in supercritical ethane, propane, butane, and CO₂. A single phase exists at conditions above each of the curves and two phases exist below the curves. The ethane, propane, and CO₂ curves represent cloud points. However, the entire butane curve represents bubble points that are very close to the vapor pressure of pure butane.

~16 000 psia in ethane, to 7000 psia in propane, to 2000 psia in butane. Dispersion interactions, which roughly scale with polarizability, α ,¹⁵ increase as the size of the SCF solvent increases from ethane ($\alpha = 4.4 \text{ \AA}^3$) to propane ($\alpha = 6.3 \text{ \AA}^3$) to butane ($\alpha = 8.1 \text{ \AA}^3$), which follows the decrease in cloud-point pressures observed in Figure 4. Note that for the butane system the transitions at 60 °C and lower are bubble points that superimpose with the butane vapor pressure curve. Hence, this poly(*p*-phenylene), **2d**, readily dissolves in butane at room conditions and pressures less than 100 psia. To precipitate the poly(*p*-phenylene) from solution, it is necessary to increase the temperature above 60 °C to decrease the density of butane which decreases its solvent power. The phase behavior shown in Figure 4 demonstrates that the octyl side chain on the poly(*p*-phenylene) has a significant effect on the solubility behavior of this polymer.

If the octyl side chain is fluorinated, it takes less pressure to dissolve the resulting poly(*p*-phenylene) in supercritical ethane, propane, and butane, and the fluorinated polymer **2c** readily dissolves in CO₂. Figure 5 shows that the fluoroctyl poly(*p*-phenylene)-ethane cloud-point curve, which is located at ~5000–12 000 psia lower pressures compared to the nonfluorinated octyl poly(*p*-phenylene) curve, increases in pressure as the temperature is reduced below 60 °C. The fluoroctyl poly(*p*-phenylene)-propane cloud-point curve exhibits similar behavior, but the propane curve is located at pressures as low as 800 psia. Note that the fluoroctyl poly(*p*-phenylene)-butane cloud-point curve essentially superposes onto the vapor pressure curve of pure butane and that the transitions are bubble points rather than fluid to liquid + liquid transitions.

It is possible to posit several plausible explanations for the large differences in the solubility of the octyl and fluoroctyl ester poly(*p*-phenylenes) in ethane, propane, and butane. The large fluoroctyl ester side chains are expected to inhibit chain-chain interactions since CF₂ and CF₃ groups exhibit very weak intermolecular interactions. Hence, chain aggregation is expected to be less in the fluoroctyl PPP-alkane mixtures compared to the octyl PPP-alkane mixtures. However, it is not readily apparent whether the fluorinated octyl ester side chains adopt an orientation favoring interactions with the aromatic backbone or with the alkane solvent. On the basis of molecular mechanics calculations, Vaia et al. suggested that flexibility of the PPP main chain is a direct function of side group orientation and size.²⁰ It

follows that the enhanced solubility of the fluoroethyl ester PPP in these alkane solvents could be a result of enhanced backbone distortion relative to the octyl ester PPP-alkane systems. At present, it is not possible to promote unequivocally one explanation over another for the differences in observed phase behavior for these octyl ester PPP-alkane mixtures, which certainly warrants further exploration.

Figure 5 also shows that fluoroethyl poly(*p*-phenylene) **2c** is extremely soluble in CO₂ as it only takes ~1000 psia at 25 °C to dissolve this polymer. The fluoroethyl poly(*p*-phenylene)-CO₂ cloud-point curve exhibits a positive slope and is located at pressures between 1000 and 5000 psia at temperatures from 20 to 120 °C, respectively. At temperatures near 100 °C where dispersion interactions should be the dominant force of attraction, the ethane and CO₂ curves virtually overlap even though the polarizability of ethane, 4.4 Å³, is much larger than that of CO₂, 2.7 Å³. However, Kazarian and co-workers have shown that CO₂ forms a CO₂-ester complex that is expected to increase in strength as the temperature decreases.²¹ Hence, the CO₂-ester complex provides the necessary interaction that makes polymer **2c** much more soluble in CO₂ as compared to ethane at temperatures below ~115 °C and especially as the temperature is reduced below 50 °C. It is important to note that the impact of this CO₂-ester complex is magnified at low temperatures because the solution density is very high in this region. The shape of the fluoroethyl poly(*p*-phenylene)-propane cloud-point curve in Figure 5 suggests that below 45 °C the pressures needed to dissolve fluoroethyl poly(*p*-phenylene) (**2c**) in propane increase sharply, which means that CO₂ is now a better solvent than propane. At low temperatures, polymer **2c** drops out of ethane and propane even as the pressure is increased rapidly since ester-ester polar interactions increase relative to ester-alkane solvent interactions and since the alkane solvents do not complex with the ester group. Figure 5 shows that butane is a much better solvent than CO₂ for polymer **2c** probably due to the high polarizability of butane and to the liquidlike density of butane at temperatures from 60 to 125 °C.

As previously mentioned, chain-chain interactions are expected to be reduced by the large fluoroethyl ester groups; however, chain-chain interactions are now expected to be even less in CO₂ since CO₂-fluoroalkane attractive interactions are stronger than CO₂-alkane interactions as surmised from phase behavior studies.¹² CO₂ interacts with the ester group on the side chain, and CO₂-aromatic, quadrupole-quadrupole interactions are favored at low temperatures.¹⁵ Hence, chain aggregation is anticipated to be less with CO₂ than with the alkane solvents. It is still not possible to ascertain whether the enhanced solubility of the fluoroethyl ester PPP in CO₂ is a result of increased chain flexibility without performing complementary light scattering studies.

Figure 6 presents a comparison of the phase behavior of the fluoroethyl poly(*p*-phenylene) (**2c**) (filled squares) obtained in this study with those previously reported for poly(1*H*,1*H*,2*H*,2*H*-tetrahydroperfluorodecyl methacrylate, filled circles),¹³ poly(1*H*,1*H*,2*H*,2*H*-tetrahydroperfluorodecyl acrylate, open squares),²² and poly(1*H*,1*H*-dihydroperfluorooctyl acrylate, open circles)²³ in supercritical CO₂. The two acrylate cloud-point curves superpose with the fluoroethyl poly(*p*-phenylene) curve which

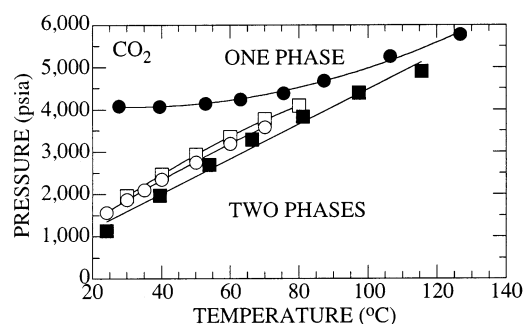


Figure 6. Comparison of the phase behavior of fluoroethyl poly(*p*-phenylene) (**2c**) (filled squares) obtained in this study with that of poly(1*H*,1*H*,2*H*,2*H*-tetrahydroperfluorodecyl methacrylate, filled circles),¹³ poly(1*H*,1*H*,2*H*,2*H*-tetrahydroperfluorodecyl acrylate, open squares),²² and poly(1*H*,1*H*-dihydroperfluorooctyl acrylate, open circles)²³ in supercritical CO₂.²³ The polymer concentrations are between 1.0 and 4.0 wt %.

suggests that the side chain on the poly(*p*-phenylene) acts as a tethered solvent that fixes the location of the curve. At temperatures greater than ~80 °C, the fluoromethacrylate curve also superposes with the other three curves although below 80 °C the fluoromethacrylate curve no longer superposes with the other curves, rather it exhibits a zero slope at higher pressures. At “cold” temperatures, in high-density CO₂, the CO₂-ester complex should have a large effect on the location of the cloud-point curve. The fluoroacrylate and fluoromethacrylate curves diverge from one another since the methyl group on a methacrylate α -carbon more effectively repels CO₂ due to both steric hindrance and repulsive interactions than does the hydrogen on an acrylate α -carbon. Hence, CO₂ has more restricted access to the ester group in the methacrylate polymer than in the acrylate polymer. In fact, Rindfleisch and co-workers have shown that, at room temperature, poly(methyl acrylate) (PMA) dissolves in CO₂ at a pressure that is more than 24 000 psia greater than that needed to dissolve poly(vinyl acetate) (PVAc) due to the easier access CO₂ has to the ester group in PVAc compared to PMA.¹⁰ At temperatures greater than ~80 °C, where the strength of the CO₂-ester complex is weaker, all of the cloud-point curves superpose, suggesting that the phase behavior is governed primarily by nonspecific dispersion interactions. The phase behavior in Figure 6 shows that CO₂ is a poor quality solvent that responds to modest variations in the chemical architecture of the polymer that changes the strength or type of intermolecular interactions.

Conclusions

From a synthetic point of view, a series of fluorinated and nonfluorinated ester substituted PPPs were successfully prepared and fully characterized. It is clear from a comparison of NMR spectral and SEC data for polymers **2a**–**2d** that we can tailor molecular weight through the addition of varying amounts of end cap; however, there remains a substantial amount of polymer terminus that is not due to the added end cap. Work is continuing to optimize synthetic procedures in order to attain greater control over end-group composition in the new fluorinated and nonfluorinated PPPs.

The results from the present study also demonstrate that the derivatized PPP polymers can be dissolved in SCF solvents at modest operating conditions which provides the opportunity for SCF-assisted processing schemes for these novel materials. For example, CO₂

can be used to process the fluoro-derivatized PPP polymers at pressures as low as 1000 psia at 25 °C, solubility conditions that are a strong function of the length of the alkoxy chain on the fluoroester substituent group. Interestingly, CO₂ can distinguish fluorinated poly(methacrylate)s from fluorinated poly(acrylate)s, which demonstrates the sensitivity CO₂ exhibits to modest variations in the chemical architecture of the polymer. The SCF solubility studies reported here follow many of the trends previously reported on the solution behavior of functionalized, rodlike polymers^{7,8} in liquid organic solvents. Further work is in progress to ascertain the physics underlying the enhanced solubility of the fluoro-octyl ester PPP relative to the octyl ester PPP in SCF solvents.

Experimental Section

General Methods. All manipulations of compounds and solvents were done under nitrogen using standard Schlenk line techniques. Triethylamine (CaH₂) and THF (Na⁺) were purified from by distillation under nitrogen from the specified drying agents. ¹H NMR and ¹³C NMR measurements were performed using one of the following instruments: Bruker AC 200 MHz, Varian Mercury 300 MHz, or Varian Inova 400 MHz spectrometer. ¹H NMR and ¹³C NMR chemical shifts are reported vs the respective solvent residue peak (solvent, ¹H, ¹³C signals: CDCl₃, δ 7.25 ppm, δ 76.9 ppm; DMSO-*d*₆, δ 2.62 ppm, δ 36.9 ppm, respectively). The octyl and propyl 2,5-dichlorobenzoate esters were prepared by standard Fischer esterification techniques. The 2,5-dichlorobenzoic acid, octanol, propanol, pentafluoropropanol, triphenylphosphine, NMP (stored over molecular sieves), and CDI were purchased from Aldrich Chemical Co. and used as received. The zinc (powder, 97%) was purchased for Fisher Scientific and used as received. The nickel bromide (anhydrous, 97%) was purchased for Alfa Chemical Co. and used as received. The CF₃(CF₂)₅CH₂CH₂OH was purchased from Apollo Scientific. DSC and TGA experiments were carried out on Perkin-Elmer DSC-7 and TGA-7 system under a nitrogen atmosphere at a flow rate of 40 cm³ N₂/min. Typical samples of 5–10 mg were run through several heating cycles to identify reproducible and distinct *T*_g/*T*_{melt} events. SEC analyses were performed by dilution in THF (2 mg/mL) and then injection onto a Hewlett-Packard 1100 HPLC (column: PL 300 × 7.5 mm, 5 μm particle size). Molecular weights are calculated relative to polystyrene standards. Elemental analyses were performed at Atlantic Microlab Inc., Norcross, GA.

Described elsewhere is the apparatus and techniques used to obtain polymer–SCF phase behavior data.^{24,25} The main component of the experimental apparatus is a high-pressure, variable-volume cell (Nitronic 50, 7.0 cm o.d. × 1.6 cm i.d., ~30 cm³ working volume). The cell is first loaded with a measured amount of polymer to within ±0.002 g. To remove entrapped air, the cell is degassed very slowly at pressures less than 40 psi with the supercritical solvent of interest. Gas is then transferred into the cell gravimetrically to within ±0.02 g using a high-pressure bomb. The mixture in the cell is viewed with a borescope (Olympus Corporation, model F100-024-000-55) placed against a sapphire window secured at one end of the cell. A stir bar activated by a magnet located below the cell mixes the contents of the cell. The solution temperature is held to within ±0.3 °C, as measured with a type K thermocouple. A fixed polymer concentration of approximately 2 wt % is used for each constant-concentration, phase boundary curve. The mixture in the cell is compressed to a single phase, and the pressure is then slowly decreased until a second phase appears. The transition is a cloud point if the solution becomes so opaque that it is no longer possible to see the stir bar in solution. These cloud points have been compared in our laboratories to those obtained using a laser light setup where the phase transition is the condition of 90% reduction in light transmitted through the solution. Both methods gave identical results within the reproducibility of the data. The cloud-point

transitions at this concentration are expected to be close to the maximum in the pressure–composition isotherms.^{26–28} The transition is a bubble point if small gas bubbles appear in the cell when the pressure is decreased. The gas phase is expected to be essentially pure solvent, and the composition of the predominant phase in the cell will equal the overall solution composition since the mass in the bubble is negligible. The system pressure is measured with Heise pressure gauges accurate to within ±10 psi for data to 10 000 psig and to within ±50 psi for data from 10 000 to 40 000 psig. Cloud points are reproduced two to three times to within approximately ±60 psi, and bubble points are also reproduced two to three times to within approximately ±20 psi.

Synthesis of Pentafluoropropyl 2,5-Dichlorobenzoate (1a). A reaction vessel was charged with CH₂Cl₂ (11 mL), 2,5-dichlorobenzoic acid (1.10 g, 5.75 mmol), pentafluoropropanol (0.86 g, 5.75 mmol, 0.6 mL), and 1,1-carbonyldiimidazole (0.93 g, 5.8 mmol). The solution was stirred at ambient temperature for 24 h, diluted with diethyl ether (50 mL), washed with H₂O (2 × 50 mL), and dried with MgSO₄, and the solvents were removed under reduced pressure. The crude product was purified by Kugelrohr distillation (~0.5 Torr) to afford **1a** as a clear and colorless oil (1.26 g, 68%). ¹H NMR (CDCl₃): δ 7.84 (s, 1H), 7.43 (s, 2H), 4.78 (t, *J* = 12.9 Hz, 2H). ¹³C NMR (CDCl₃): δ 162.2, 133.8, 133.3, 133.1, 132.8, 132.6, 131.9, 118.2 (CF₂), 116.8 (CF₃), 60.3. IR (neat): ν_{CO} 1755 cm⁻¹. Anal. Calcd for C₁₀H₅Cl₂F₅O₂: C, 37.18; H, 1.56. Found: C, 37.12; H, 1.51.

Synthesis of Tridecafluorooctyl 2,5-Dichlorobenzoate (1c). A reaction vessel was charged with CH₂Cl₂ (10 mL), 2,5-dichlorobenzoate (2.41 g, 12.6 mmol), 1,1-carbonyldiimidazole (2.00 g, 12.6 mmol), and tridecafluorooctanol (2.78 mL, 4.58 g, 12.6 mmol) and stirred at ambient temperature for 24 h. The solution was diluted with ether (75 mL), washed with H₂O (2 × 100 mL), dried with MgSO₄, filtered, and concentrated to yield a yellow liquid. The crude product was purified by Kugelrohr distillation (~0.5 Torr) to afford **1c** as a clear and colorless oil (4.72 g, 76%). ¹H NMR (CDCl₃): δ 7.79 (s, 1H), 7.37 (s, 2H), 4.62 (t, *J* = 4.8 Hz, 2H), 2.70–2.50 (m, 2H). ¹³C NMR (CDCl₃): δ 164.0, 133.1, 132.9, 132.6, 132.5, 131.6, 130.5, 122–105 (multiple signals for CF₂'s), 57.73 (OCH₂), 30.58 (CF₃). IR (neat): ν_{CO} 1740 cm⁻¹. Anal. Calcd for C₁₅H₇Cl₂F₁₃O₂: C, 33.55; H, 1.32. Found: C, 34.22; H, 1.32.

Polymerization of Pentafluoropropyl 2,5-Dichlorobenzoate (2a). To a charged flask of NMP (~14 mL), pentafluoropropyl 2,5-dichlorobenzoate (6.56 g, 20.3 mmol), methyl 3-chlorobenzoate (0.346 g, 2.03 mmol), and PPh₃ (2.13 g, 8.12 mmol) were heated to 80 °C. After 5 min, NiBr₂ (0.437 g, 2.03 mmol) and Zn (2.65 g, 40.6 mmol) were added simultaneously to the mixture and heated at 80 °C for 2 h. The oil bath was removed, and the mixture was allowed to cool to ambient temperature and then diluted with CH₂Cl₂ (50 mL). The mixture was filtered through celite, washed with H₂O (2 × 100 mL) and NaCN (5% aqueous solution, 100 mL), dried over MgSO₄, and then concentrated to a volume of ~5 mL under reduced pressure. The concentrated polymer solution was precipitated into cold MeOH (75 mL). The product was collected by filtration and dried under reduced pressure to afford **2a** as a white solid (3.41 g, 66%, *M*_n = 15 400, PD = 1.98). ¹H NMR (CDCl₃): δ 8.31–8.14 (m), 8.01, 7.66, 7.54, 7.46, 4.79, 3.94, 3.37, 2.36. ¹³C NMR (CDCl₃): δ 165.5, 132.9, 132.3, 131.5, 131.2, 129.3, 129.1, 110.0 (CF₂), 59.5 (CH₂), 51.2 (CF₃). IR (neat): ν_{CO} 1734 cm⁻¹. UV–vis (THF): λ_{max} = 318 nm. Anal. Calcd for (C₁₀H₅O₂F₅)_{*n*}: C, 46.21; H, 2.01. Found: C, 46.13; H, 2.34.

Polymerization of Propyl 2,5-Dichlorobenzoate (2b). A NMP (~6 mL) solution containing propyl 2,5-dichlorobenzoate (2.41 g, 10.3 mmol), PPh₃ (1.09 g, 4.14 mmol), and methyl 3-chlorobenzoate (0.18 g, 1.03 mmol) was heated to 80 °C under a nitrogen atmosphere. After 5 min, NiBr₂ (0.23 g, 1.03 mmol) and Zn (1.35 g, 20.66 mmol) were added simultaneously, and the solution was heated at 80 °C for 2 h with stirring. The polymer was isolated as above to afford **2b** as a white powder (1.3 g, 78%, *M*_n = 8400, PD = 2.15). ¹H NMR (CDCl₃): δ 8.40, 8.25, 8.05, 7.57, 7.48, 4.25, 4.11–4.10 (m), 3.93 (s, 3H), 2.54 (s), 0.78 (s). ¹³C NMR (CDCl₃): δ 168.3, 133.2,

131.7, 131.0, 130.8, 130.5, 129.0, 67.2, 21.9, 10.6. IR (neat): ν_{CO} 1720 cm^{-1} . UV-vis (THF): $\lambda_{\text{max}} = 310$ nm. Anal. Calcd for $(\text{C}_{10}\text{H}_{10}\text{O}_2)_n$: C, 73.95; H, 6.19. Found: C, 73.95; H, 6.09.

Polymerization of Tridecafluorooctyl 2,5-Dichlorobenzoate (2c). A solution of NMP (~6 mL) containing tridecafluorooctyl 2,5-dichlorobenzoate (4.98, 9.27 mmol), PPh_3 (0.97, 3.71 mmol), and methyl 3-chlorobenzoate (0.16 g, 0.93 mmol) was heated to 80 °C for 5 min. Then NiBr_2 (0.20 g, 0.93 mmol) and Zn (1.21 g, 18.5 mmol) were added simultaneously to the mixture and heated at 80 °C for 2 h. Work-up and isolation as above afforded **2c** as a white solid (2.52 g, 58%, $M_n = 7200$, PD = 1.65). ^1H NMR (CDCl_3): br s at with some fine structure at δ 8.35, 8.24–8.21, 8.06–8.04, 7.94–7.89, 7.51, 4.64, 4.42–4.35, 3.97, 3.91, 2.61, 2.29, 1.55. ^{13}C NMR (CDCl_3): δ 167.4, 141.1, 133.0, 132.2, 130.7, 129.4, 128.9, 121.8, 120.5, 117.5, 113.5, 111.1, 105.0. IR (neat): ν_{CO} 1645 cm^{-1} . $\lambda_{\text{max}} = 305$ nm. Anal. Calcd for $(\text{C}_{15}\text{H}_7\text{F}_{13}\text{O}_2)_n$: C, 39.84; H, 1.66. Found: C, 39.63; H, 1.69.

Polymerization of Octyl 2,5-Dichlorobenzoate (2d). A reaction vessel was charged with NMP (8 mL), octyl 2,5-dichlorobenzoate (3.84 g, 12.7 mmol), triphenylphosphine (1.33 g, 5.1 mmol), and methyl 3-chlorobenzoate (0.21 g, 1.27 mmol) was heated to 80 °C. After 5 min nickel(II) bromide (0.27 g, 1.27 mmol) and zinc (1.66 g, 25.4 mmol) were added to the solution. The solution was heated with stirring for 2 h at 80 °C. Work-up and isolation as above afforded **2d** as a white solid (2.1 g, 71%, $M_n = 13\,200$, PD = 2.1). ^1H NMR (CDCl_3): δ 7.94 (s, 1H), 7.55, 4.12 (s), 4.04 (s), 1.46 (s, 3H), 1.21 (s, 10H), 0.84 (s, 3H). ^{13}C NMR (CDCl_3): δ 168.3, 141.2, 131.7, 131.2, 130.7, 130.4, 129.1, 128.9, 65.7, 32.0, 29.4, 28.9, 28.5, 26.0, 22.8, 14.3. IR (neat): 1717 cm^{-1} . UV-vis (CH_2Cl_2): $\lambda_{\text{max}} = 315$ nm. Anal. Calcd for $(\text{C}_{15}\text{H}_{20}\text{O}_2)_n$: C, 77.39; H, 8.62. Found: C, 77.14; H, 8.37.

References and Notes

- Busch, H.; Weber, W.; Darboven, C.; Renner, W.; Hahn, H.; Mathause, G.; Startz, F.; Zitzmann, K.; Engelhardt, H. *J. Prakt. Chem.* **1936**, *146*, 1.
- Stille, J. K.; Gilliams, Y. *Macromolecules* **1971**, *4*, 515. VanKerckhoven, H. F.; Gilliams, Y. K.; Stille, J. K. *Macromolecules* **1972**, *5*, 541 and references therein.
- Hamaguchi, M.; Sawada, H.; Kyokane, J.; Yoshino, K. *Chem. Lett.* **1996**, 527. Gin, D. L.; Conticello, V. P. *Trends Polym. Sci.* **1996**, *4*, 217. Percic, V.; Hill, D. H. *ACS Symp. Ser.* **1996**, *624*, 2.
- Kovacic, P.; Jones, M. B. *Chem. Rev.* **1987**, *87*, 357 and references therein. Percic, V.; Okita, S.; Weiss, R. *Macromolecules* **1992**, *25*, 1816–1823. Percic, V.; Zhao, M.; Bae, J.-Y.; Hill, D. H. *Macromolecules* **1996**, *29*, 3727. Wang, Y.; Quirk, R. P. *Macromolecules* **1995**, *28*, 3495. Goodson, F. E.; Wallow, T. I.; Novak, B. M. *Macromolecules* **1998**, *31*, 2047. Havelka-Rivard, P. A.; Nagai, K.; Freeman, B. D.; Sheares, V. V. *Macromolecules* **1999**, *32*, 6418. Schlüter, A. D. *J. Polym. Sci., Part A: Polym. Chem.* **2001**, *39*, 1533.
- Chaturvedi, V.; Tanaka, S.; Kaeriyama, K. *Macromolecules* **1993**, *26*, 2607. Kaeriyama, K.; Mehta, M. A.; Masuda, H. *Synth. Met.* **1995**, *69*, 507. Kaeriyama, K.; Mehta, M. A.; Chaturvedi, V.; Masuda, H. *Polymer* **1995**, *36*, 3027.
- Marrocco, M. L.; Gagne, R. R.; Trimmer, M. S. U.S. Patent 5,756,581, 1998. Marrocco, M. L.; Gagne, R. R.; Trimmer, M. S. U.S. Patent 5,565,543, 1996. Marrocco, M. L.; Gagne, R. R.; Trimmer, M. S. U.S. Patent 5,227,457, 1993.
- Ballauff, M. *Fluid Phase Equilib.* **1993**, *83*, 349. Ballauff, M. *Angew. Chem., Int. Ed. Engl.* **1989**, *28*, 253.
- Galda, P.; Kistner, D.; Martin, A.; Ballauff, M. *Macromolecules* **1993**, *26*, 1595. Vaia, R. A.; Krishnamoorti, R.; Benner, C.; Trimer, M. *J. Polym. Sci., Part B: Polym. Phys.* **1998**, *36*, 2449.
- Park, K. C.; Dodd, L. R.; Levon, K.; Kwei, T. K. *Macromolecules* **1996**, *29*, 7149. Vaia, R. A.; Dudis, D.; Henes, J. *Polymer* **1998**, *39*, 6021.
- Rindfleisch, F.; DiNoia, T. P.; McHugh, M. A. *J. Phys. Chem.* **1996**, *100*, 15581.
- Sarbu, T.; Styranec, T. J.; Beckman, E. J. *Ind. Eng. Chem. Res.* **2000**, *39*, 4678.
- Kirby, C. F.; McHugh, M. A. *Chem. Rev.* **1999**, *99*, 565 and references therein.
- McHugh, M. A.; Garach-Domech, A.; Park, I. H.; Barbu, E.; Graham, P.; Tsibouklis, J. *Macromolecules* **2002**, *35*, 6479.
- McHugh, M. A.; Krukonic, V. *Supercritical Fluid Extraction: Principles and Practice*, 2nd ed.; Butterworth-Heinemann: Boston, 1994.
- Prausnitz, J. M.; Lichtenthaler, R. N.; de Azevedo, E. G. *Molecular Thermodynamics of Fluid-Phase Equilibria*, 3rd ed.; Prentice Hall: Englewood Cliffs, NJ, 1999.
- Gottikh, B. P.; Krayevsky, A. A.; Tarusova, N. B.; Purygin, P. P.; Tsilevich, T. L. *Tetrahedron* **1970**, *26*, 4419.
- Colon, I.; Kelsey, D. R. *J. Org. Chem.* **1986**, *51*, 2627.
- Care should be taken when using sodium cyanide solutions, and all work should be done in a hood with adequate air flow and with the appropriate chemical lab ware.
- Because of the rigid nature of PPPs, GPC results (using polystyrene standards) will lead to "inflated" molecular weight values and degrees of polymerization: Holdcroft, S. *J. Polym. Sci., Part B: Polym. Phys.* **1991**, *29*, 1585.
- In ref 9 the work of Vaia et al. suggests that backbone distortion induced from side chain interaction is important in describing polymer structure. Park and co-workers (ref 9) suggest that the overall orientation of the side chains (cylindrical vs "plain plate structure") is primary to describing polymer structure.
- Kazarian, S. G.; Vincent, M. F.; Bright, F. V.; Liotta, C. L.; Eckert, C. A. *J. Am. Chem. Soc.* **1996**, *118*, 1729.
- Mawson, S.; Johnston, K. P.; Combes, J. R.; DeSimone, J. M. *Macromolecules* **1995**, *28*, 3182.
- Luna-Barcenas, G.; Mawson, S.; Takishima, S.; DeSimone, J. M.; Sanchez, I. C.; Johnston, K. P. *Fluid Phase Equilib.* **1998**, *146*, 325.
- Meilchen, M. A.; Hasch, B. M.; McHugh, M. A. *Macromolecules* **1991**, *24*, 4874.
- Mertdogan, C. A.; Byun, H.-S.; McHugh, M. A.; Tuminello, W. H. *Macromolecules* **1996**, *29*, 6548.
- Allen, G.; Baker, C. H. *Polymer* **1965**, *6*, 181.
- Irani, C. A.; Cozewith, C. *J. Appl. Polym. Sci.* **1986**, *31*, 1879.
- Lee, S.-H.; LoStracco, M. A.; Hasch, B. M.; McHugh, M. A. *J. Phys. Chem.* **1994**, *98*, 4055.

MA021615E